

RESEARCH

Open Access



The multifaceted role of vitreous hyalocytes: Orchestrating inflammation, angiomodulation and erythrophagocytosis in proliferative diabetic retinopathy

Stefaniya K. Boneva^{1*}, Julian Wolf¹, Malte Jung¹, Gabriele Prinz¹, Toco Y. P. Chui², Jacqueline Jauch¹, Anne Drougard^{3,4}, J. Andrew Pospisilik^{3,4}, Anja Schlecht^{1,5,6}, Felicitas Bucher¹, Richard B. Rosen², Hansjürgen Agostini¹, Günther Schlunck¹ and Clemens A. K. Lange^{1,7*}

Abstract

Background Despite great advances in proliferative diabetic retinopathy (PDR) therapy over the last decades, one third of treated patients continue to lose vision. While resident vitreous macrophages called hyalocytes have been implicated in the pathophysiology of vitreoretinal proliferative disease previously, little is known about their exact role in PDR. In this study, we address molecular and cellular alterations in the vitreous of PDR patients as a means towards assessing the potential contribution of hyalocytes to disease pathogenesis.

Results A total of 55 patients were included in this study encompassing RNA-Sequencing analysis of hyalocytes isolated from the vitreous of PDR and control patients, multiplex immunoassay and ELISA analyses of vitreous samples from PDR and control patients, as well as isolation and immunohistochemical staining of cultured porcine hyalocytes. Transcriptional analysis revealed an enhanced inflammatory response of hyalocytes contributing to the cytokine pool within the vitreous of PDR patients by expressing interleukin-6, among others. Further, increased angiopoietin-2 expression indicated that hyalocytes from PDR patients undergo a proangiogenic shift and may thus mediate the formation of retinal neovascularizations, the hallmark of PDR. Finally, RNA-Sequencing revealed an upregulation of factors known from hemoglobin catabolism in hyalocytes from PDR patients. By immunohistochemistry, cultured porcine hyalocytes exposed to red blood cells were shown to engulf and phagocytose these, which reveals hyalocytes' potential to dispose of erythrocytes. Thus, our data suggest a potential role for vitreous macrophages in erythrophagocytosis and, thereby, clearance of vitreous hemorrhage, a severe complication of PDR.

Conclusion Our results strongly indicate a critical role for vitreous hyalocytes in key pathophysiological processes of proliferative diabetic retinopathy: inflammation, angiomodulation and erythrophagocytosis. Immunomodulation of hyalocytes may thus prove an essential novel therapeutic approach in diabetic vitreoretinal disease.

*Correspondence:

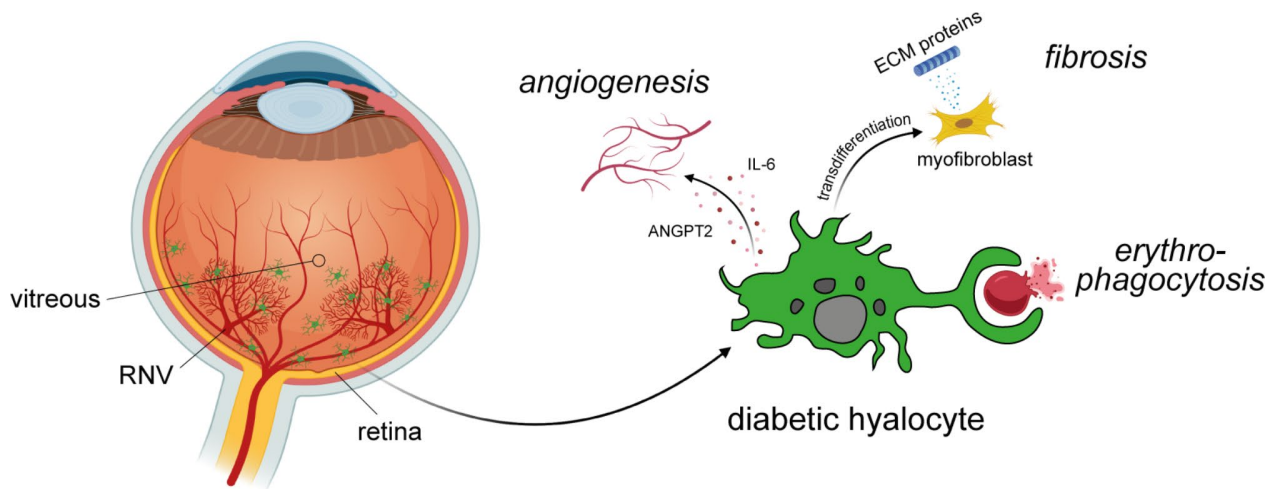
Stefaniya K. Boneva
stefaniya.boneva@uniklinik-freiburg.de
Clemens A. K. Lange
clemens.lange@augen-franziskus.de

Full list of author information is available at the end of the article



© The Author(s), corrected publication 2024. **Open Access** This article is licensed under a Creative Commons Attribution 4.0 International License, which permits use, sharing, adaptation, distribution and reproduction in any medium or format, as long as you give appropriate credit to the original author(s) and the source, provide a link to the Creative Commons licence, and indicate if changes were made. The images or other third party material in this article are included in the article's Creative Commons licence, unless indicated otherwise in a credit line to the material. If material is not included in the article's Creative Commons licence and your intended use is not permitted by statutory regulation or exceeds the permitted use, you will need to obtain permission directly from the copyright holder. To view a copy of this licence, visit <http://creativecommons.org/licenses/by/4.0/>.

Graphical Abstract



In the left-hand side panel, a human eye of a patient with proliferative diabetic retinopathy with retinal neovascularizations (RNV) growing in the preretinal vitreous is schemed. Hyalocytes, the macrophages of the vitreous, are located mainly in the posterior part of the eye, close to the vitreo-retinal interface and, thus, RNV. Diabetic hyalocytes (on the right) modulate angiogenesis by expressing factors such as interleukin-6 (IL-6) and angiopoietin-2 (ANGPT2), contribute to fibrosis by transdifferentiation in myofibroblasts secreting extracellular matrix (ECM) components, and participate in erythrophagocytosis, as shown in this study

Keywords Hyalocytes, Vitreous macrophages, Proliferative diabetic retinopathy, Inflammation, Angiomodulation, Erythrophagocytosis, RNA-Sequencing

Background

Diabetic retinopathy (DR) is a leading cause of blindness worldwide, with a global prevalence estimated to 93 million people in 2012 [1] projected to nearly triple in the USA by 2050 [2]. Proliferative DR (PDR), the advanced stage of the disease, is marked by areas of reduced retinal perfusion that generate an uncontrolled release of proangiogenic growth factors eventually leading to the formation of vulnerable new blood vessels called “retinal neovascularizations” (RNV, [3]). The compensatory attempts at revascularization of the ischemic retina generally result in unfavorable angiogenesis towards vitreous [4], the stimulus for this pathological preretinal formation of contractile vascular membranes remaining the matter of debate. Evidentially, a major driver of neovascularization in PDR is the vascular endothelial growth factor (VEGF) targeted effectively in routine treatment of diabetic macular edema (DME) and PDR by the application of anti-VEGF antibodies or decoy antibody receptors [5]. More recently, faricimab, a bispecific antibody acting as an inhibitor of both VEGF and angiopoietin-2 (ANGPT2), was introduced to enhance treatment for neovascular eye disease [6]. Those successes notwithstanding, other pathways likely contribute to PDR pathogenesis, as the disease often progresses even under continuous anti-VEGF therapy [7] and addition

of ANGPT2 inhibition has improved outcomes in only a minority of DME patients switched from aflibercept [8]. A deeper understanding of additional mechanisms underlying PDR development is therefore critical for unveiling alternative therapeutic options, given the disease’s growing socio-economic impact.

Clinical evidence clearly demonstrates that the vitreous is critically involved in PDR, as florid preretinal neovascularization in PDR is mitigated following posterior vitreous detachment (PVD, [9]) and generally does not recur post-vitreectomy [10]. It appears likely that additional components of the vitreous, other than the supporting structure of vitreal collagen fibers, are involved. Recent evidence suggests that hyalocytes, the vitreous resident myeloid cells [11, 12], may be essential participants in the course of proliferative vitreoretinal disease. Hyalocytes are distributed largely within the vitreous cortex abutting the retinal surface [13], in immediate proximity to RNV sites. We have previously demonstrated in a RNV mouse model that myeloid cells cluster in the vicinity of RNV [14] and may influence their formation [15]. Moreover, transcriptional and single-cell protein analysis of human RNV have revealed an abundance of antigen-presenting cells, most likely hyalocytes, which bear the potential of myofibroblastic transdifferentiation [16]. Finally, advanced in vivo imaging techniques have identified

macrophage-like cells (MLC) accumulating around RNV in the vitreoretinal interface (VRI) of DR patients [17]. While these observations are suggestive, the exact role of vitreous hyalocytes in the pathophysiology of PDR remains largely unknown.

In this study, we report a high-dimensional molecular characterization of hyalocytes from the diabetic vitreous compared to controls performed with the aim to better assess their potential role in PDR pathophysiology. Our transcriptional analysis reveals enhanced inflammatory responses by hyalocytes, which appear to contribute, as a so far underestimated factor, to the cytokine pool within the PDR vitreous. The data further indicate an expression shift in hyalocytes in PDR towards a proangiogenic phenotype, suggesting they may mediate RNV formation. This could explain the misdirected growth of RNV towards the preretinal vitreous and alleviated RNV formation following vitrectomy. Finally, our data suggest a role of vitreous macrophages in erythrophagocytosis and removal of vitreous hemorrhage (VH) debris. The results of our study may pave the way for novel immunomodulatory approaches in the treatment of end-stage diabetic vitreoretinal disease.

Materials and methods

Patients' characteristics

A total of 55 patients were included in this study. Only patients with no history of previous vitreoretinal surgery, concurrent vitreoretinal disease, or anti-VEGF therapy within the last three months were enrolled. Three control patients had type II diabetes without evidence of DR.

Adaptive optics scanning light ophthalmoscopy (AOSLO) imaging was performed on two patients (a 32-year-old healthy control [18] and a 26-year-old PDR patient [17]), as described previously [18]. The other 53 patients underwent vitrectomy for complications of PDR, macular pucker (MP) or macular hole (MH) between 2018 and 2021 (demographics and clinical characteristics summarized in Tables 1 and 2). RNA-Sequencing (RNA-Seq) analysis was performed on 21 samples from 30 patients (Tbl. 1). In order to exclude possible confounding effects of Red Blood Cell (RBC) lysis buffer treatment on the expression profile of vitreous hyalocytes, four pooled samples were processed for a preliminary analysis. For each final sample, the vitreous specimens of three to four MP or MH patients were pooled, divided in two equal halves and either subject to lysis (" + lysis", similar to diabetic samples in the main analysis) or analyzed without lysis treatment (" - lysis", Tbl. 1). Eight samples from eight patients with PDR (mean age 57 ± 15.4 years) were compared to nine control samples from nine patients (MP and MH, mean age 75 ± 6.2 years) in the main analysis.

For protein analysis by enzyme-linked immunosorbent assay (ELISA) or multiplex immunoassay, 31 undiluted vitreous samples were obtained at the start of vitrectomy (before intraocular fluid infusion) from the mid-vitreous of 23 patients (samples from eight patients were processed for both readouts) and centrifuged at $500 \times g$ for 20 min at 4°C . Corresponding plasma specimens were collected before or during surgery by peripheral venous puncture, centrifuged ($3000 \times g$ for 15 min at 4°C) and, like vitreous samples, stored at -80°C until processing.

Ethics approval was granted by the local Ethics Committee and a written informed consent was obtained from each patient prior to surgery. All research adhered to the tenets of the Declaration of Helsinki.

Fluorescence-activated cell sorting (FACS)

Vitreous tissue samples were collected in vitrectomy bags during surgery and processed for cell isolation within two hours of resection, according to a previously published protocol [11] adapted for the specificities of diabetic vitreous. For half of the samples in the preliminary analysis (see Table 1) and for diabetic samples, 1 ml of RBC lysis buffer (Thermo Fisher Scientific) was added for erythrocyte lysis. Samples were stained for cluster of differentiation (CD) 45 (BV421, anti-human, 1:100, BioLegend), CD11b (FITC, anti-human, 1:100, BioLegend), CX₃C motif chemokine receptor 1 (CX₃CR1, PE-Cy7, anti-human, 1:200, BioLegend), and with the anti-human Mature Macrophages (MatMac) antibody, an ED2-like (ectodermal dysplasia 2) marker for resident macrophages (eFluor660, anti-human, 1:100, eBioscience). Finally, cells were processed for sorting on the MoFlo Astrios EQ Cytometer (Beckman Coulter). Hyalocytes were isolated as CD45⁺CD11b⁺CX₃CR1⁺MatMac⁺ cells.

Total RNA extraction and RNA-Seq library preparation

RNA extraction, library preparation and RNA-Seq were conducted at the Genomics Core Facility "KFB - Center of Excellence for Fluorescent Bioanalytics" (University of Regensburg, Germany), according to previously published protocols [11, 16].

Bioinformatics

Sequencing data were analyzed on the Galaxy web platform (usegalaxy.eu [19]), as previously described by our group [20]. Transcripts with log₂ fold change (log₂FC) > 2 or < -2 and adjusted *p*-value < 0.05 were considered differentially expressed genes (DEG). Gene ontology (GO) analysis for clusters related to biological processes (BP) was performed based on all DEG in hyalocytes from PDR patients vs. controls.

Table 1 Characteristics of patient samples included in RNA-Sequencing analysis

Preliminary analysis										
Sam- ple #	Age	Sex	DM Type	Ocular Diagnosis	VH	TRD	Relevant systemic disorders	Lens status	PVD	Previous anti-VEGF treatment
1	83	F	NA	MP	NA	NA	asthma	phakic	no	NA
	68	M	II	MP	NA	NA	-	phakic	no	NA
	69	F	NA	MP	NA	NA	-	phakic	no	NA
	79	F	NA	MP	NA	NA	-	phakic	yes	NA
2	68	F	NA	MP	NA	NA	-	phakic	no	NA
	76	F	NA	MP	NA	NA	asthma, st. p. fibromyalgia, st. p. borreliosis	phakic	no	NA
	78	F	NA	MP	NA	NA	-	phakic	no	NA
	61	F	NA	MH	NA	NA	-	phakic	no	NA
3	74	F	NA	MP	NA	NA	st. p. chemotherapy for breast carcinoma, Parkinson's	phakic	no	NA
	82	M	NA	MP	NA	NA	-	phakic	no	NA
	81	F	NA	MP	NA	NA	rheumatoid arthritis	pseudophakic	yes	NA
	67	F	NA	MP	NA	NA	-	phakic	no	NA
4	76	F	NA	MH	NA	NA	-	phakic	no	NA
Main analysis										
Sam- ple #	Age	Sex	DM Type	Ocular Diagnosis	VH	TRD	Relevant systemic disorders	Lens status	PVD	Previous anti-VEGF treatment
5	77	M	II	PDR	+	+	-	phakic	no	no
6	40	M	I	PDR	+	+	-	phakic	no	yes
7	56	M	II	PDR	+	+	-	phakic	no	no
8	29	F	I	PDR	+	+	-	phakic	no	no
9	66	F	II	PDR	+	-	-	pseudophakic	yes	> 3 months
10	62	M	I	PDR	-	+	st. p. kidney and pancreas transplantation	pseudophakic	no	yes
11	63	M	II	PDR	+	+	renal insufficiency	phakic	no	no
12	64	F	II	PDR	+	-	-	pseudophakic	no	yes
13*	79	F	II	MP	NA	NA	asthma	pseudophakic	no	NA
14	72	M	NA	MP	NA	NA	-	pseudophakic	yes	NA
15	73	M	NA	MP	NA	NA	-	pseudophakic	no	NA
16	73	F	NA	MP	NA	NA	fibromyalgia	pseudophakic	no	NA
17*	68	M	NA	MH	NA	NA	psoriasis	phakic	no	NA
18	88	M	NA	MH	NA	NA	-	pseudophakic	no	NA

Sam-
ple #

Age

Sex

DM Type

Ocular
Diagnosis

VH

TRD

Relevant systemic disorders

Lens status

PVD

Previous anti-VEGF treatment

Cell count

RNA concentration (pg/ μ l)

+/- lysis

90/264

71/116

94/86

104/154

79/139

84/11

139/147

43/85

280

38

2300

322

980

49

1800

82

454

68

723

64

1077

211

512

86

944

109

291

142

464

161

701

73

424

73

315

301

Table 1 (continued)

19	78	F	NA	MH	NA	st. p. giant cell arteritis, celiac disease	phakic	yes	NA	NA	550	110
20	69	M	NA	MH	NA	-	phakic	no	NA	NA	164	174
21	72	F	NA	MH	NA	-	pseudophakic	no	NA	NA	240	78

DM, diabetes mellitus. VH, vitreous hemorrhage. TRD, tractional retinal detachment. PVD, posterior vitreous detachment. VEGF, vascular endothelial growth factor. PRP, periretinal photocoagulation. RNA, ribonucleic acid. NA, not applicable. MP, macular pucker. MH, macular hole. PDR, proliferative diabetic retinopathy. Two control samples (one MP and one MH, marked by an asterisk here) analyzed in a previous study [11] were processed anew and their newly generated transcriptional profiles compared to the data of the old sequencing batch. As no batch effect was present between the samples from the first analysis and the newly available sequencing profiles (data not shown), transcriptional data of the published control group of nine samples was processed for this study, too

Multiplex immunoassay

Cytokine levels were measured in vitreous and corresponding plasma samples from nine PDR (mean age 45±14.7 years) and 10 MH (control) patients (mean age 62±14.8 years, Tbl. 2). A multiplex electrochemiluminescence assay (V-Plex Human Biomarker 54-Plex Kit, Meso Scale Discovery) was used according to manufacturer’s instructions. By combination of electrochemiluminescence and multi-array technologies, the levels of 54 cytokines were simultaneously measured including interleukin (IL)-6, IL-8, IL-15, monocyte chemoattractant protein 1 (MCP-1), placental growth factor (PlGF), VEGF-A. This panel was selected to assess the expression of factors previously identified as relevant in the progression of PDR or DEG in hyalocytes from PDR patients based on the RNA-Seq results of this study. For statistical analysis, all values below the detection limit were assigned to half the respective values of the detection limit.

Enzyme-linked immunosorbent assay (ELISA)

Vitreous and plasma levels of ANGPT2 were measured in samples from six PDR (mean age 44±18.2 years) and six MH (control) patients (mean age 66±8.5 years, Tbl. 2) with the Human Angiopoietin-2 Quantikine ELISA (R&D Systems) according to manufacturer’s instructions.

Cultivation and staining of porcine hyalocytes

Porcine eyes were obtained from a local abattoir. In terms of development, anatomy and morphology, these are considered representative for the human situation [21]. Vitreous was extracted from six eyes and placed in Dulbecco’s Modified Eagle Medium (DMEM, Gibco). On the next day, peripheral blood was obtained from healthy human donors by venous puncture and centrifuged at 3000 rpm for 10 min at 4 °C to obtain erythrocytes. One drop of erythrocyte concentrate was added to each vitreous sample. On day 3, specimens were fixed in methanol for 10 min at -20 °C prior to blocking for one hour at room temperature (RT) in a solution of 1% bovine serum albumin (Roth) and 5% normal donkey serum (Biozol) in phosphate-buffered saline Triton-X 0.1% (Gibco). For immunohistochemistry (IHC), cells were incubated with ionized calcium-binding adapter molecule 1 (IBA-1, abcam) and CD235a (Thermo Fischer Scientific) primary antibodies for one hour at RT. Primary antibodies were omitted for negative control. Incubation with secondary antibodies (Alexa 647, Life Technologies; Alexa 488, Invitrogen) and Phalloidin 5(6)-Tetramethylrhodaminisothiocyanate (TRITC, Sigma-Aldrich) was performed for one hour at RT. Nuclei were counterstained with 4’,6-Diamidin-2-phenylindol (DAPI) prior to embedding in Fluorescence Mounting Medium (Agilent Dako). Representative images were taken on a Leica TCS

Table 2 Characteristics of patient samples included in protein analysis

ELISA												
Sample #	Age	Sex	DM Type	Ocular Diagnosis	VH	TRD	Relevant systemic disorders	Lens status	PVD	Previous anti-VEGF treatment	Previous PRP treatment	
1	28	M	I	PDR	+	+	-	phakic	no	no	yes	
2	20	F	I	PDR	+	+	-	phakic	yes	no	yes	
3	61	M	I	PDR	+	+	renal insufficiency	pseudophakic	no	no	yes	
4	45	F	II	PDR	+	+	renal insufficiency	phakic	no	> 3 months	yes	
5	45	F	II	PDR	+	+	-	phakic	no	no	no	
6	67	F	II	PDR	+	+	-	phakic	no	no	yes	
7	70	F	NA	MH	NA	NA	-	phakic	no	NA	NA	
8	66	M	NA	MH	NA	NA	-	phakic	no	NA	NA	
9	72	M	NA	MH	NA	NA	-	phakic	no	NA	NA	
10	49	F	NA	MH	NA	NA	-	phakic	no	NA	NA	
11	69	F	NA	MH	NA	NA	st. p. thyroidectomy for thyroid cancer	phakic	no	NA	NA	
12	69	M	NA	MH	NA	NA	st. p. cryogenic pneumonia	phakic	no	NA	NA	
Multiplex protein analysis												
Sample #	Age	Sex	DM Type	Ocular Diagnosis	VH	TRD	Relevant systemic disorders	Lens status	PVD	Previous anti-VEGF treatment	Previous PRP treatment	
13	35	M	I	PDR	+	+	renal insufficiency	phakic	no	no	yes	
14	64	M	II	PDR	-	-	-	phakic	no	> 3 months	yes	
15	52	F	II	PDR	+	+	-	phakic	no	no	yes	
16	41	M	I	PDR	+	+	-	phakic	no	no	yes	
17	20	F	I	PDR	+	+	-	phakic	yes	no	yes	
18	33	M	I	PDR	+	+	-	phakic	no	> 3 months	yes	
19	61	M	I	PDR	+	+	renal insufficiency	pseudophakic	no	no	yes	
20	58	F	II	PDR	+	+	-	phakic	no	no	yes	
21	45	F	II	PDR	+	+	renal insufficiency	phakic	no	> 3 months	yes	
22	24	F	NA	MH	NA	NA	-	phakic	no	NA	NA	
23	62	F	NA	MH	NA	NA	-	phakic	no	NA	NA	
24	69	F	NA	MH	NA	NA	-	phakic	no	NA	NA	
25	67	F	NA	MH	NA	NA	Graves' disease	phakic	no	NA	NA	
26	66	M	NA	MH	NA	NA	-	phakic	no	NA	NA	
27	72	M	NA	MH	NA	NA	-	phakic	no	NA	NA	
28	49	F	NA	MH	NA	NA	-	phakic	no	NA	NA	
29	71	F	II	MH	NA	NA	possible giant cell arteriitis, renal insufficiency	pseudophakic	yes	NA	NA	
30	69	F	NA	MH	NA	NA	st. p. thyroidectomy for thyroid cancer	phakic	no	NA	NA	
31	69	M	NA	MH	NA	NA	st. p. cryogenic pneumonia	phakic	no	NA	NA	

DM, diabetes mellitus. VH, vitreous hemorrhage. TRD, tractional retinal detachment. PVD, posterior vitreous detachment. VEGF, vascular endothelial growth factor. PRP, panretinal photocoagulation. PDR, proliferative diabetic retinopathy. NA, not applicable. MH, macular hole

SP8 Confocal System coupled to a Leica DMi8 inverted microscope.

Statistical analysis

Statistical analysis was performed using GraphPad Prism (GraphPad Software, Version 10.2.3). For multiplex immunoassay analysis, one-way ANOVA and subsequent multiple comparison testing was performed. For ANGPT2 expression analysis by ELISA, a Mann-Whitney test was applied. The following significance levels were considered: * $p < 0.05$, ** $p < 0.01$, *** $p < 0.001$, **** $p < 0.0001$.

Results

Analysis workflow

Diagnosis for the 55 included patients was based on a thorough funduscopic exam (Fig. 1A), spectral domain optical coherence tomography (OCT) and fluorescence angiography (FA, HRA2, Heidelberg Engineering) for PDR patients (Fig. 1A'). Samples from 30 patients undergoing vitrectomy for PDR, MP or MH were processed for RNA-Seq analysis (Tbl. 1). Hyalocytes were isolated from vitreous tissue by flow cytometry (Figs. 1B, [11]) specifically targeting resident immune cells by utilizing, among others, the MatMac marker for tissue-specific

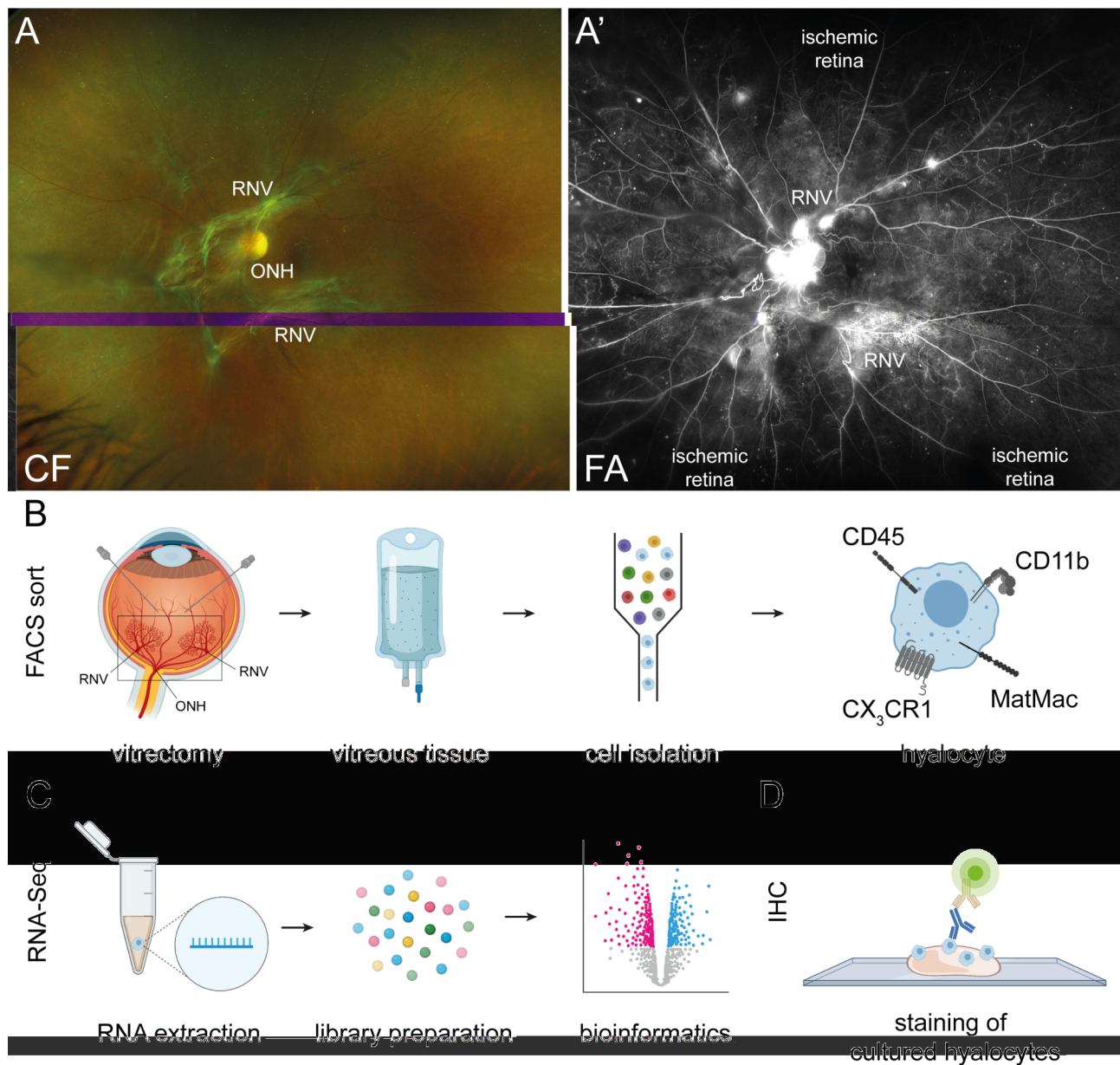


Fig. 1 Experimental workflow. Diagnosis was based on a thorough fundoscopic exam documented by fundus photography (CF, color fundus, **A**), spectral domain optical coherence tomography (OCT) and fluorescence angiography (FA, **A'**), for proliferative diabetic retinopathy (PDR) patients (black areas are not sufficiently supplied with blood and therefore ischemic). **B**. Vitreous samples were obtained by vitrectomy from PDR and control patients. The black rectangle is to illustrate the part of the bulb imaged by CF in **A**, and FA in **A'**. Hyalocytes were isolated from vitreous tissue by flow cytometry (fluorescence-activated cell sorting, FACS) as $CD45^+CD11b^+CX3CR1^+MatMac^+$ cells and were further processed for **C**. RNA extraction and library preparation. RNA-Sequencing (RNA-Seq) data were analyzed bioinformatically. **D**. For visualization of hyalocytes, porcine vitreous tissue was cultured and stained by immunohistochemistry (IHC). ONH, Optic nerve head. RNV, retinal neovascularization

macrophages. This antibody was applied to exclude any potential contamination with blood-derived monocytes owing to possible surgically induced microbleeds, as infiltrating leukocytes generally lack the antigen [22, 23]. In the following, sorted hyalocytes were analyzed by RNA-Seq (Fig. 1C). Staining by IHC was performed on hyalocytes (Fig. 1D) isolated from porcine vitreous tissue. MLC in the VRI of a healthy control and a PDR patient

imaged by AOSLO are shown in Fig. 2 and Additional File 1.

Effect of RBC lysis on the transcriptional profile of human hyalocytes

In our study, RBC lysis proved indispensable for isolation of hyalocytes from the blood-tinged diabetic vitreous, but unnecessary to process control vitreous. Furthermore, a

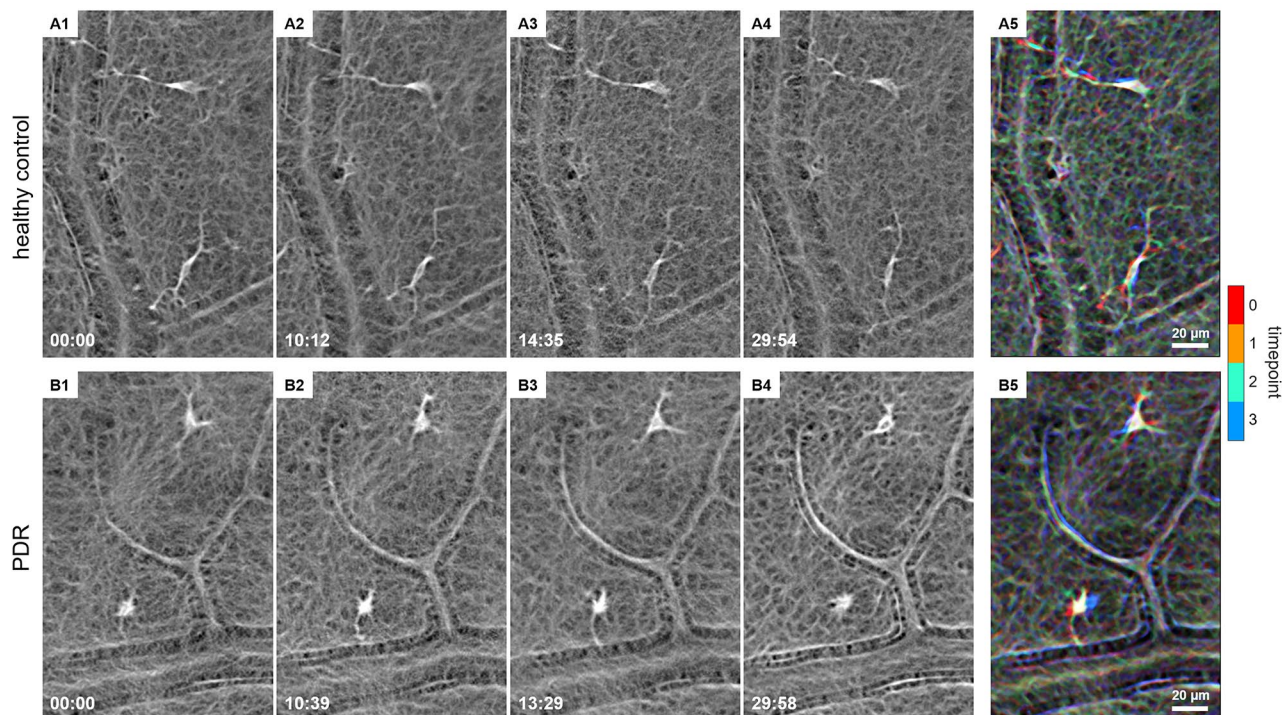


Fig. 2 Adaptive optics scanning light ophthalmoscopy (AOSLO) imaging of macrophage-like cells in the vitreoretinal interface. Two adjacent hyalocytes with different movement behaviors over 30 min of AOSLO imaging in (top row, **A1–A4**; modified from [18]) a 32-year-old healthy control and (bottom row, **B1–B4**) a 26-year-old proliferative diabetic retinopathy (PDR) patient. **A5 & B5**. Chromo-temporal map composites of the four time points over 30 min, which indicate movement of cell bodies and processes across the imaging period. Time of acquisition in the lower-left corner is displayed in mins:secs. A video of the entire imaging region of interest, which includes these four cells, is shown in Additional File 1

lysis-induced reduction of cell count in single non-diabetic samples under the limit of feasible transcriptional analysis was observed in preparation for this study.

Although lysed samples in our preliminary analysis showed a trend to a lower cell count (mean count: 100.5 ± 26.4 cells vs. 159.0 ± 75.1 cells, $p=0.22$) and lower RNA concentration (mean concentration: 75.5 ± 25.6 pg/ μ l vs. 91.5 ± 60.6 pg/ μ l, $p=0.65$), no distinct effect of lysis on the RNA profile of hyalocytes could be inferred, as highlighted by the conducted principal component analysis (PCA, Additional File 2A) and heatmap visualization (Additional File 2B). Based on the negligible effect of RBC lysis treatment on hyalocyte transcriptional data, further analysis was performed comparing lysed diabetic samples and non-lysed control samples (MP and MH). MP and MH hyalocytes are considered comparable in their transcriptional signature [11], which prompted us to process them together.

Transcriptional profiling of human diabetic hyalocytes

Diabetic samples tended to yield a higher amount of hyalocytes in comparison to control samples (1015.8 ± 703.6 vs. 454.8 ± 246.8 cells, $p=0.063$), while mean concentration of RNA extracted from isolated hyalocytes was comparable (115.0 ± 99.3 vs. 135.7 ± 72.5 pg/ μ l, $p=0.636$). A

mean total number of 43.7 million (± 4.3) raw reads per sample was obtained from diabetic hyalocytes, while 37.8 million (± 6.5) raw reads per sample were detected for control hyalocytes ($p=0.045$).

A total of 43,278 transcripts with at least one read in at least one sample were obtained. PCA revealed clear separation of diabetic and control hyalocytes' transcriptomes on the first two principle components indicating substantial differences between the two groups (Fig. 3A). Despite within-group heterogeneity visible in the generated DEG heatmap, a distinct pattern of transcriptome differences was evident between both entities (Fig. 3B). Comparative analysis of the transcriptome of diabetic and control hyalocytes revealed 126 differentially upregulated and 222 differentially downregulated genes in diabetic samples relative to controls (Fig. 3C). Notably, among the most strongly upregulated genes in diabetic hyalocytes ranked a number of factors implicated in inflammatory (cathepsin (CTS) B (*CTSB*), *CTSL*, *CTSD* and S100 calcium-binding protein A8 (*S100A8*)), but also anti-inflammatory responses (ferritin light chain, *FTL*), or both (legumain (*LGMN*)).

To gain more insight into BP diabetic hyalocytes are involved in, we performed a GO cluster analysis of all DEG (Fig. 3D). According to our data, DEG mostly

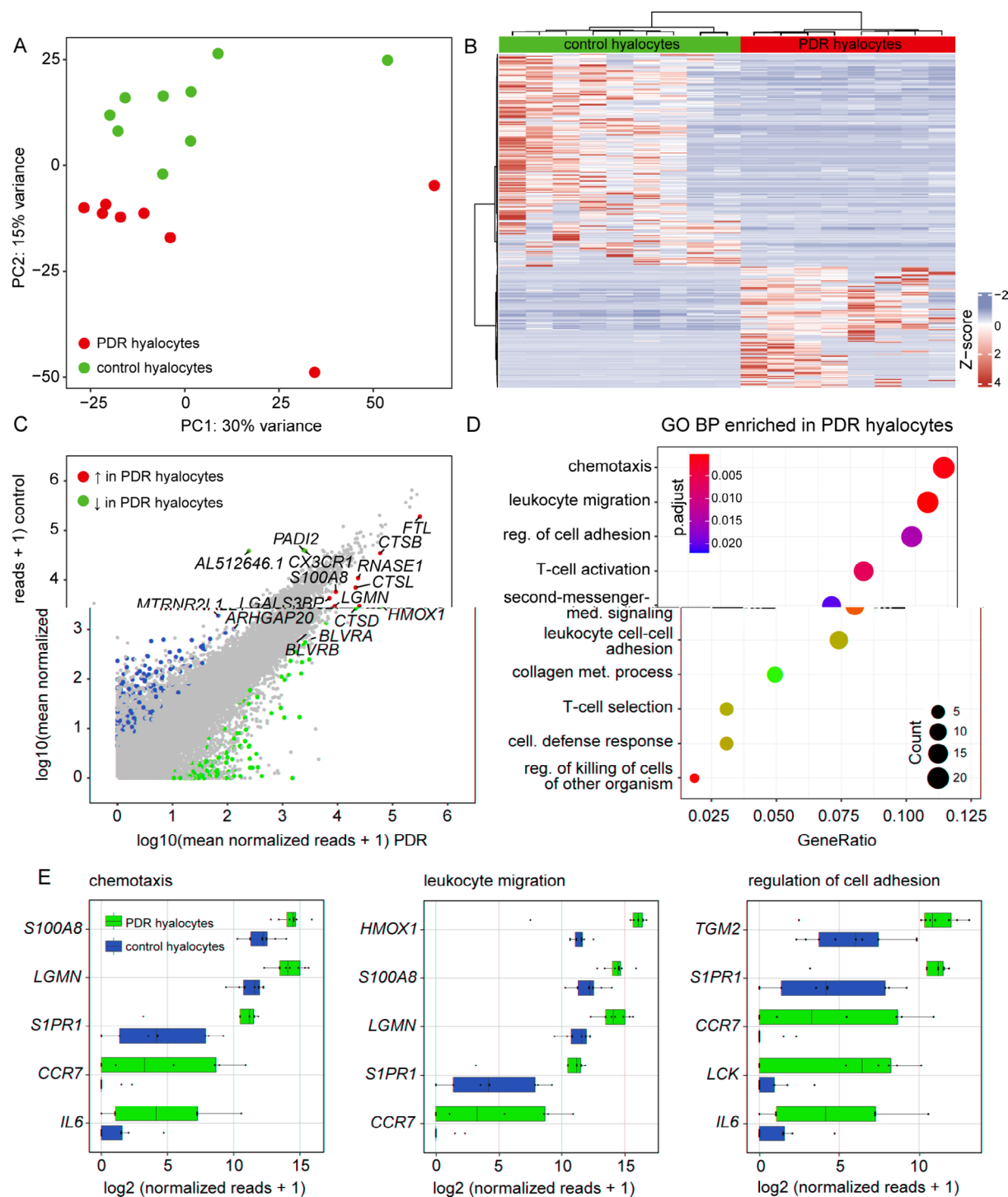


Fig. 3 Transcriptional signature of diabetic hyalocytes. **(A)** A Principal Component Analysis (PCA) plot demonstrates the distribution of hyalocyte samples isolated from the vitreous of patients with PDR (red dots) and control samples (green dots). **(B)** Heatmap of differentially expressed genes (DEG, $\log_2FC > 2$, adjusted p value < 0.5 , sorted according to the \log_2FC) between hyalocytes isolated from the vitreous of PDR patients and control hyalocytes. Color coding of the transcripts according to the z-score (deviation from a gene's mean expression in standard deviation units). **(C)** Readplot of DEG in diabetic hyalocytes (upregulated genes in red, downregulated genes in green, not differentially expressed genes in grey; the most strongly expressed genes from each group are labeled; also labeled are the biliverdin reductases A and B, *BLVRA* and *BLVRB*). **(D)** Top 10 most significantly upregulated Gene Ontology (GO) biological process (BP) clusters on the basis of all DEG in diabetic hyalocytes. Color coding of the dots according to the adjusted p value, size of the dots according to the count of transcripts associated with the respective GO term. **(E)** Top five most highly expressed transcripts in the three most enriched GO terms from D

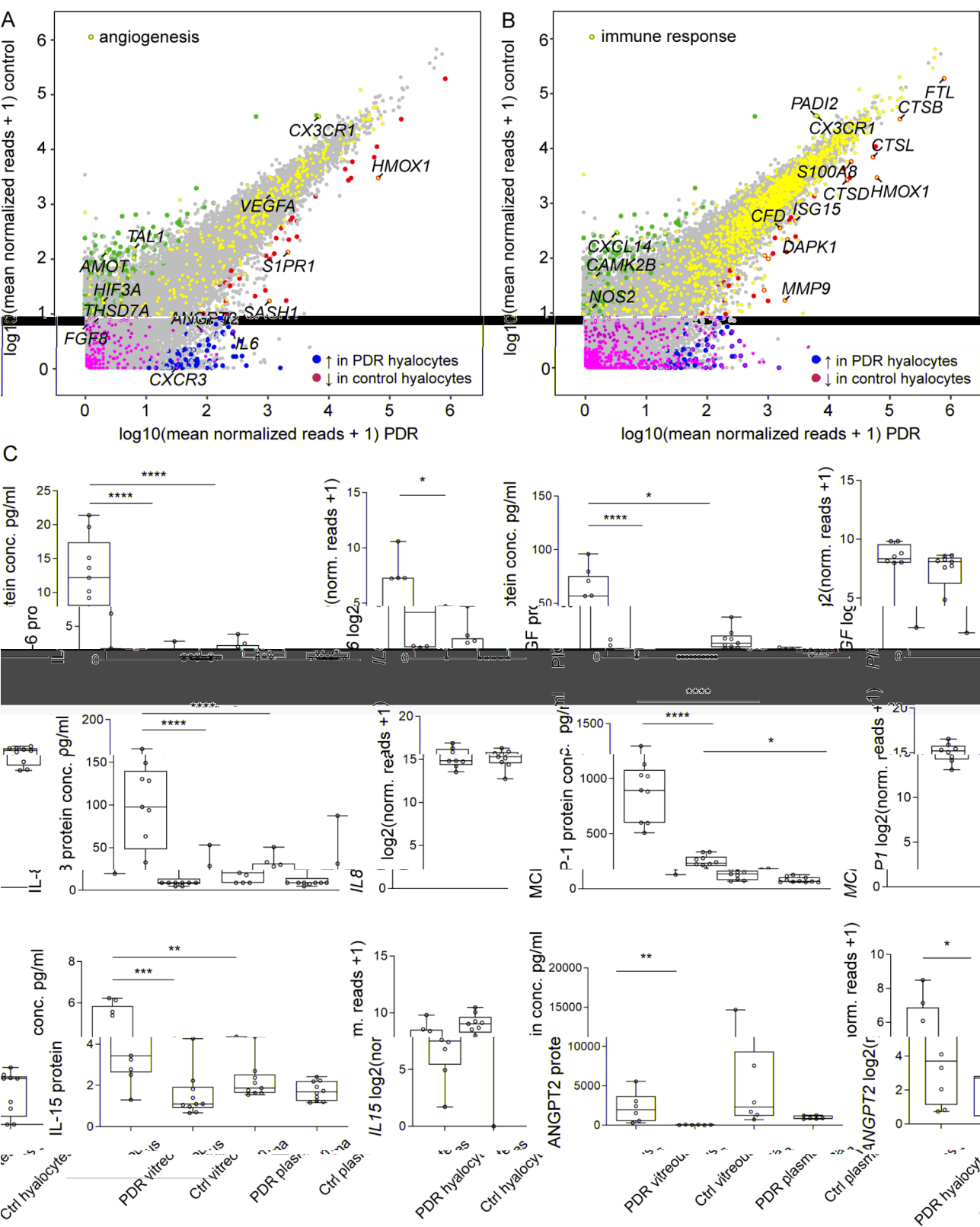


Fig. 4 (See legend on next page.)

(See figure on previous page.)

Fig. 4 “Angiogenesis” and “immune response”-associated genes expressed in hyalocytes from proliferative diabetic retinopathy (PDR) patients. **(A)** Readplot of differentially expressed genes (DEG) in diabetic hyalocytes (upregulated genes in red, downregulated genes in green, not differentially expressed genes in grey; factors associated with the Gene Ontology (GO) biological process (BP) “angiogenesis” are highlighted in yellow; the most strongly upregulated “angiogenesis”-related genes are labeled). **(B)** Readplot of DEG in diabetic hyalocytes (upregulated genes in red, downregulated genes in green, not differentially expressed genes in grey; factors associated with the GO BP “immune response” are highlighted in yellow; the most strongly upregulated “immune response”-related genes are labeled). **(C)** Left-hand side panels show boxplots for multiplex immunoassay analysis of interleukin (IL)-6, placental growth factor (PIGF), IL-8, monocyte chemoattractant protein-1 (MCP-1) and IL-15 protein expression or enzyme-linked immunosorbent analysis (ELISA) of angiopoietin-2 (ANGPT2) protein expression in PDR vitreous and plasma and control (Ctrl) vitreous and plasma samples. * $p < 0.05$, ** $p < 0.01$, *** $p < 0.001$, **** $p < 0.0001$ (one-way ANOVA and consequent analysis of multiple comparisons conducted for multiplex immunoassay analysis and Mann-Whitney-Test performed for ELISA analysis). Corresponding gene expression analysis for *IL6*, *PIGF*, *IL8*, *MCP1* (= *CCL2*), *IL8* (= *CXCL8*) and *ANGPT2* in PDR and control hyalocytes is shown on the right, respectively

contributed to processes like “chemotaxis” (GO:0006935) and “leukocyte migration” (GO:0050900), but also “regulation of cell adhesion” (GO:0030155) and “collagen metabolic process” (GO:0032963). *S100A8* was the most highly expressed factor in the cluster “chemotaxis” and the second-most highly expressed factor in “leukocyte migration” (Fig. 3E).

Since angiogenesis and immune response are key processes in the pathogenesis of PDR [24], we took a closer look at genes involved in both processes. We found heme oxygenase 1 (*HMOX1*) involved in hemoglobin catabolism, but also *IL6* and angiopoietin-2 (*ANGPT2*) to be among the most strongly expressed factors in “angiogenesis” in hyalocytes from PDR patients (Fig. 4A). For “immune response”, besides the already established factors *FTL*, *CTSB*, *CTSL*, *CTSD* and *S1008*, matrix metalloproteinase 9 (*MMP9*) was among the PDR-associated factors in hyalocytes that stood out (Fig. 4B).

Protein analysis

According to the multiplex immunoassay, IL-6, which was overexpressed in PDR hyalocytes on the RNA level ($\log_2FC = 4.24$, adjusted $p = 0.01$), was also strongly enriched in PDR vitreous in comparison to control vitreous and when compared to corresponding plasma on the protein level (Fig. 4C). PIGF was also significantly upregulated in PDR vitreous in comparison to both control vitreous and corresponding plasma. However, these changes did not correspond to a significant enrichment of the respective gene in diabetic hyalocytes ($\log_2FC = 0.83$, adjusted $p = 0.74$, Fig. 4C). The same was the case for IL-8 ($\log_2FC = 0.17$, adjusted $p = 0.97$), MCP-1 ($\log_2FC = 0.25$, adjusted $p = 0.95$) and IL-15 ($\log_2FC = -1.00$, adjusted $p = 0.72$, Fig. 4C). VEGF was detected on the protein level by two assays, which both demonstrated an upregulation in the diabetic vitreous when compared to control vitreous (** $p < 0.01$). In one of the assays, an upregulation against corresponding plasma of PDR patients was detected (** $p < 0.01$). Of note, gene expression of *VEGFA* did not differ significantly between hyalocytes isolated from the PDR and control vitreous, indicating that other ocular cell types are likely the source of increased VEGF protein levels in the diabetic vitreous.

As assessed by ELISA, *ANGPT2*, a DEG in PDR hyalocytes when compared to control hyalocytes ($\log_2FC = 3.57$, adjusted $p = 0.01$), was significantly upregulated in the PDR vitreous in comparison to control vitreous, too (Mann-Whitney test, Fig. 4C).

Erythrophagocytosis in hyalocytes

According to our transcriptional analysis, *HMOX1*, an important factor in heme catabolism [25, 26], was one of the most highly expressed genes in diabetic hyalocytes when compared to control hyalocytes. This prompted us to elucidate further marker genes of erythrophagocytosis and iron regulator genes [25, 27] in the data set. Beside *FTL* and *HMOX1*, ferritin heavy chain 1 (*FTH1*) was also significantly upregulated in diabetic hyalocytes. Other factors, such as the biliverdin reductases A and B (*BLVRA* and *BLVRB*), showed a trend (*BLVRA*: $\log_2FC = 1.78$, adjusted $p = 0.30$, *BLVRB*: $\log_2FC = 1.42$, adjusted $p = 0.32$) towards an enrichment in PDR hyalocytes (Figs. 2C and 5A).

In order to assess the potential of hyalocytes to phagocytose erythrocytes, as suggested by our sequencing results, we next examined cultured porcine hyalocytes. Hyalocytes seemed to engulf erythrocytes, which could clearly be distinguished within the Phalloidin-stained cytoskeleton of the immune cells. Within the cytoplasm of IBA1-positive hyalocytes, we observed vesicles containing CD235a-stained, most probably erythrocyte debris, but also DAPI-positive particles to be considered digested nuclei (Fig. 5B). Negative controls are shown in Additional File 3 (for IBA-1: A., for CD235a: B.). These data suggest that hyalocytes have the potential to remove damaged erythrocytes, which may be of critical importance for diabetic VH clearance.

Discussion

More than one third of PDR cases deteriorate despite complete panretinal photocoagulation or continuous anti-VEGF treatment [28]. Thus, investigation of the molecular and cellular mechanisms underlying end-stage DR pathophysiology is indispensable to prevent severe vision loss. In this study, we performed an in-depth transcriptional characterization of hyalocytes isolated from

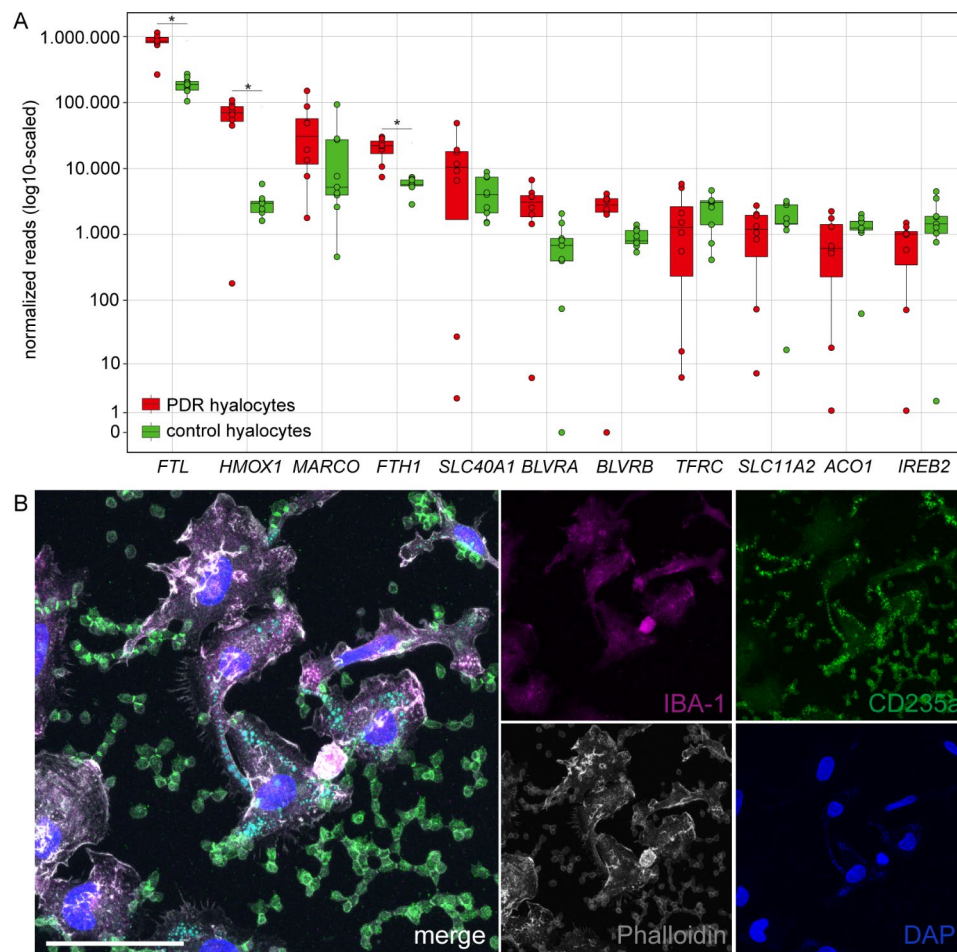


Fig. 5 Erythrophagocytosis in hyalocytes. **(A)** Boxplots of the expression of marker genes of erythrophagocytosis and iron regulator genes in proliferative diabetic retinopathy (PDR, red) and control (green) hyalocytes. * $p < 0.05$. **(B)** Immunohistochemical staining of cultured porcine hyalocytes for ionized calcium-binding adaptor molecule 1 (IBA-1), cluster of differentiation 235a (CD235a) and Phalloidin. Nuclei are counterstained with 4',6-Diamidin-2-phenylindol (DAPI). Within the cytoplasm of hyalocytes, vesicles containing CD235a- (= erythrocyte debris), but also DAPI-stained particles (= digested nuclei) were observed. Scale bar corresponds to 50 μ m

the vitreous of PDR patients to assess the role of this specialized immune cell population in disease progression. We demonstrate that hyalocytes contribute to a proinflammatory and proangiogenic milieu in the diabetic vitreous by expressing several cytokines but may also play a role in VH clearance. In addition to a presumed role in tractional retinal detachment (TRD) by hyalocyte-to-myofibroblast transdifferentiation, as suggested by us previously [16], our current data implicate the importance of hyalocytes in angiogenesis and red blood cell cleanup, two further hallmarks of vision-threatening PDR.

The transcriptional analysis of 43,278 genes revealed a distinct expression signature of diabetic hyalocytes when compared to control hyalocytes. GO cluster analysis demonstrated that DEG in diabetic hyalocytes mainly contribute to processes like “chemotaxis” and “leukocyte migration” highlighting the importance of innate immune responses in the course of severe vitreoretinal disease.

The more active immunological state of PDR hyalocytes was supported by AOSLO imaging of hyalocytes, which in PDR appeared amoeboid-shaped in comparison to the slender, ramified and quiescent MLC in a healthy patient. Besides, DEG were enriched in processes like “regulation of cell adhesion” and “collagen metabolic process”, which suggests an involvement of diabetic hyalocytes in wound repair and would be in line with previous findings on hyalocyte-to-myofibroblast transdifferentiation in PDR [16].

Next, we examined closely two key pathways in PDR pathophysiology – angiogenesis and immune response. In contrast to *VEGFA*, *IL6* and *ANGPT2* were among the most strongly enriched factors for the term “angiogenesis” in hyalocytes from PDR patients suggesting these cells as an origin for proinflammatory and proangiogenic cytokines in the diabetic vitreous. IL-6 has been previously shown to be enriched in the diabetic vitreous [29], which may correspond to disease severity [30]. In

our study, IL-6 was strongly overexpressed in PDR vitreous samples in comparison to control vitreous and corresponding plasma, which implies a local production by vitreal and/or retina cells. The potential of IL-6 signaling inhibition is currently being explored in experimental and clinical trials for the treatment of DR-related complications [31]. *ANGPT2* also lined among the “angiogenesis”-related DEG in diabetic hyalocytes. The factor is known from routine clinical practice with the application of the faricimab antibody [32]. An overexpression of *ANGPT2* in the diabetic vitreous on the protein level has been previously demonstrated [33] and was confirmed here. For other analytes, too, such as PIGF, IL-8, MCP-1, and IL-15, a strong upregulation in PDR vitreous samples when compared to control vitreous and corresponding plasma was detected, which is in line with previously published data [29, 34, 35]. However, these factors were not significantly enriched in diabetic hyalocytes implying alternative cell populations as the source for their abundance in the vitreous. It should further be critically considered that various cells of the retina known to express IL-6 (fibroblasts and pericytes) and *ANGPT2* (endothelial cells, [36]) in the steady state more pronouncedly than hyalocytes may be the major contributors of both factors to the diabetic vitreous.

Among the 126 differentially upregulated genes in hyalocytes from PDR patients, several proinflammatory factors, such as *CTSB*, *CTSL*, *CTSD* and *S100A8*, stood out. Cathepsins have previously been implied in mediating an inflammatory response in macrophages, e.g. in carotid plaques [37], adipose tissue [38] and inflammatory bowel disease [39]. *S100A8*, together with *S100A9*, encodes for the S100A8/A9 protein complex calprotectin and its expression is upregulated in human choroidal neovascularization tissue [40]. Myeloid cells including macrophages express S100A8/A9 constitutively, while in inflammation, secretion of the protein is enhanced and known to stimulate cytokine release [41]. Inhibition of S100A8/A9 alleviates excessive cytokine production, which reveals its potential as a therapeutic target [42]. In addition, *FTL*, which has previously been determined as the second-most prominent transcript in human control hyalocytes [11], ranked among the top expressed factors in diabetic hyalocytes, also, with a much higher expression in the disease state. *FTL* encodes the light subunit of the ferritin protein, the main iron storage in the human body previously associated with anti-inflammatory responses in murine macrophages [43]. Since an iron overload and subsequent susceptibility to oxidative damage has been described for the PDR vitreous [44], it is tempting to speculate about a role of hyalocyte-derived *FTL* in neuroprotective iron reduction in the vitreous.

On another note, potential deleterious effects of activated hyalocytes in PDR conveyed by the expression of

inflammatory and angiogenic factors such as IL-6 and *ANGPT2* may well be in contrast to beneficial features of this cell population known, similarly to microglia, for its dual nature [45]. Along these lines, our transcriptional analysis revealed an upregulation of factors known from hemoglobin catabolism, such as *HMOX1*, *BLVRA* and *BLVRB*, in diabetic hyalocytes. The notion of hyalocytes' phagocytic activity has been suggested as early as in the middle of the 20th century by Hamburg, who assumed that hyalocytes contribute to clearance of metabolic products [46]. By state-of-the-art imaging, hyalocytes have been shown here and previously [18] to continuously scan the environment with their protrusions in anticipation of harmful signals. Upon detection of danger, hyalocytes are likely to migrate and phagocytose the pathogen, akin to microglia of the central nervous system and in accordance with recent evidence that hyalocytes express factors important for phagocytosis, such as *MERTK* (MER proto-oncogene, tyrosine kinase), *CD74* and MHCII-associated genes (major histocompatibility complex class II, [11]). To assess hyalocytes' potential to phagocytose erythrocytes, we exposed cultured porcine hyalocytes to erythrocytes and subsequently stained them for CD235a, an abundant protein in erythrocyte membranes. Our data demonstrate the capacity of hyalocytes to engulf and dispose of erythrocytes, a process known as erythrophagocytosis. Hereby, damaged/senescent erythrocytes are removed from circulation primarily by macrophages in the spleen, liver, and bone marrow [47]. For erythrocytes, CD47 is known as a “marker of self” preventing their premature clearance [48]. Further studies are needed, in order to elucidate if “eat me/don't eat me” signals [49] to hyalocytes are also conveyed CD47-dependently and how hyalocytes decide whether they are going to embrace their advantageous functions with erythrophagocytosis, or involve in pernicious cytokine release in vitreoretinal disease.

Interpretation of our data is limited by several factors, for instance the use of samples from patients with vitreoretinal disease, namely MP or MH, as controls. However, MP and MH represent the most physiological fresh samples that can be obtained in clinical routine. Another important limiting factor in our study is the age difference between PDR and control patients. While MP and MH are regarded age-related disorders of the VRI, severe PDR commonly affects younger patients. Differences in age distribution in this study should therefore be critically considered. Further, it was not possible to obtain detailed information on the preoperative extent of avascularity and degree of neovascularization for PDR patients, since FA of sufficient quality was not feasible for the majority of patients due to view obscuration by VH. Lastly, the young age of pigs serving as a source for our in vitro model could also represent a confounder. However,

since the vitreous of 8–10-month-old pigs as examined in our study, an age that in theory corresponds to human 18 years, has been reported to theoretically possess the viscoelastic properties of adult human vitreous [50], we consider this limitation negligible.

Conclusions

In conclusion, transcriptional analysis of diabetic hyalocytes, protein analysis of PDR vitreous and immunohistochemical studies on cultured hyalocytes in our work reveal an enrichment of proinflammatory and proangiogenic factors, such as *IL6* and *ANGPT2*, in hyalocytes from PDR patients, which is conveyed in an abundance of both factors in the diabetic vitreous on the protein level. Our data further suggest an important role of hyalocytes in erythrophagocytosis, which may be critical in VH clearance in PDR, especially in non-vitreotomized eyes. As hyalocytes have previously been shown to transdifferentiate to myofibroblasts, this unique cell population of the vitreous may play a role in both critical complications of PDR: vitreous hemorrhage and tractional retinal detachment. Immunomodulation of hyalocytes may thus prove an essential novel therapeutic approach in diabetic vitreoretinal disease.

Abbreviations

AOSLO	Adaptive optics scanning light ophthalmoscopy
ANGPT2	Angiotensinogen-2
BLVR	Biliverdin reductases
BP	Biological process
CD	Cluster of differentiation
CF	Color fundus
CTS	Cathepsin
CX ₃ CR1	CX ₃ C motif chemokine receptor 1
DAPI	4',6-Diamidin-2-phenylindol
DEG	Differentially expressed genes
DME	Diabetic macular edema
DMEM	Dulbecco's Modified Eagle Medium
DR	Diabetic retinopathy
ECM	Extracellular matrix
ED2	Ectodermal dysplasia 2
ELISA	Enzyme-linked immunosorbent assay
FA	Fluorescence angiography
FACS	Fluorescence-activated cell sorting
FTH1	Ferritin heavy chain 1
FTL	Ferritin light chain
GO	Gene ontology
HMOX1	Heme oxygenase 1
IBA-1	Ionized calcium-binding adaptor molecule 1
IHC	Immunohistochemistry
IL	Interleukin
LGMN	Legumain
log2FC	Log2 fold change
MatMac	Anti-human Mature Macrophages antibody
MCL	Macrophage-like cells
MCP-1	Monocyte chemoattractant protein 1
MERTK	MER proto-oncogene, tyrosine kinase
MH	Macular hole
MHCII	Major histocompatibility complex class II
MMP9	Metalloproteinase 9
MP	Macular pucker
OCT	Optical coherence tomography
ONH	Optic nerve head
PCA	Principal component analysis

PDR	Proliferative diabetic retinopathy
PIGF	Placental growth factor
PVD	Posterior vitreous detachment
S100A8	S100 calcium-binding protein A8
RBC lysis buffer	Red Blood Cell lysis buffer
RNA	Ribonucleic acid
RNA-Sequencing	RNA-Seq
rpm	Rounds per minute
RNV	Retinal neovascularization
RT	Room temperature
TRD	Tractional retinal detachment
TRITC	5(6)-Tetramethylrhodaminisothiocyanate
VEGF	Vascular endothelial growth factor
VH	Vitreous hemorrhage
VRI	Vitreoretinal interface

Supplementary Information

The online version contains supplementary material available at <https://doi.org/10.1186/s12974-024-03291-5>.

Additional File 1 (Movie,.avi). Adaptive optics scanning light ophthalmoscopy (AOSLO) time-lapse video of macrophage-like cells in the vitreoretinal interface. Two adjacent hyalocytes with different movement behaviors over 30 min of AOSLO imaging in (A) a 32-year-old healthy control and (B) a 26-year-old proliferative diabetic retinopathy (PDR) patient. Time of acquisition in the lower-left corner is displayed in mins:secs. Video is looped three times for better visualization

Additional File 2 (Figure,.tif). Impact of Red Blood Cell (RBC) Lysis on hyalocyte expression. In order to assess the effects of the RBC lysis procedure on the transcriptional profile of hyalocytes, we conducted a preliminary analysis of control samples (each pooled from the vitreous tissue of 3 to 4 patients, see Table 1), which were processed to equal parts for a treatment with and without lysis. (A) Principal Component Analysis (PCA) demonstrating distribution of the analyzed entities: samples processed with lysis ("+" lysis", dark red dots) and non-lysed samples ("-" lysis", light blue dots). The only sample in the right part of the graph was designated as a relative outlier, as less mapped reads were assigned to this sample than to other analyzed samples. (B) Unsupervised heatmap of expressed genes sorted according to mean expression in all samples

Additional File 3 (Figure,.tif). Negative controls for immunohistochemistry. For negative controls, primary antibodies were omitted. Negative control for ionized calcium-binding adaptor molecule 1 (IBA-1, A) and cluster of differentiation 235a (CD235a) immunohistochemical staining (B) shown in Fig. 5B. Nuclei are counterstained with DAPI (4',6-Diamidin-2-phenylindol). DAR647, donkey anti-rabbit Alexa Fluor 647. DAM488, donkey anti-mouse Alexa Fluor 488. Scale bars correspond to 100 µm

Acknowledgements

The authors would like to thank Thomas Ness, MD (Eye Center, University Medical Center Freiburg, Germany) for surgical assistance. Cell sorting was performed at the Lighthouse Core Facility (LCF, University of Freiburg (the LCF is funded in part by the Medical Faculty, University of Freiburg (Project Numbers 2021/A2-Fol; 2021/B3-Fol) and The German Research Foundation (Deutsche Forschungsgemeinschaft, DFG, Project Number 450392965)). Illumina deep sequencing was carried out at the Genomics Core Unit: Center of Excellence for Fluorescent Bioanalytics (KFB, University of Regensburg, Germany; www.kfb-regensburg.de).

Author contributions

SKB, JW, JAP, HA, GS and CAKL contributed to conceptualization and design of this study. SKB, JW, MJ, TYPC, GP, JJ and AD conducted experiments and data analysis. SKB, JW, TYPC, JAP, AS, FB, RBR, HA, GS and CAKL performed data interpretation. SKB and CAKL drafted the article, which was critically revised and approved by all authors.

Funding

SKB is supported by the Berta-Ottenstein-Programme for Clinician Scientists, Faculty of Medicine, University of Freiburg, the Dr. Werner

Jackstädt Foundation and the German Research Foundation (Deutsche Forschungsgemeinschaft, DFG). Open Access funding enabled and organized by Projekt DEAL.

Data availability

Sequencing data generated in this study are available in the Gene Expression Omnibus (GEO) database under accession number GSE276892. For PDR samples processed for transcriptional analysis sample numbers in this dataset correspond to annotation in Table 1. For control samples analyzed elsewhere [11], GEO accession numbers are listed here (one number for each flow cell, three flow cells per sample): sample #14: GSM4437362, GSM4437363, GSM4437364; sample #15: GSM4437365, GSM4437366, GSM4437367; sample #16: GSM4437380, GSM4437381, GSM4437382; sample #18: GSM4437368, GSM4437369, GSM4437370; sample #19: GSM4437371, GSM4437372, GSM4437373; sample #20: GSM4437374, GSM4437375, GSM4437376; sample #21: GSM4437383, GSM44373834, GSM44373835.

Declarations

Ethics approval and consent to participate

Ethics approval was granted by the local Ethics Committee and a written informed consent was obtained from each patient prior to surgery. All research adhered to the tenets of the Declaration of Helsinki.

Consent for publication

A consent for publication was granted by patients whose images and videos are shown in this study.

Competing interests

SKB and JW have previously received a speaker honorarium from Bayer Vital GmbH. CAKL is member of the Publication Steering Committee of the SPECTRUM trial by Bayer and has received a speaker honorarium from Appeli and Bayer Vital GmbH. Other than that, the authors declare that research was conducted in the absence of any commercial or financial relationships that could be construed as a potential conflict of interest.

Author details

¹Eye Center, Medical Center, Faculty of Medicine, University Medical Center Freiburg, Freiburg, Germany

²Department of Ophthalmology, New York Eye and Ear Infirmary of Mount Sinai, Icahn School of Medicine at Mount Sinai, New York, NY, USA

³Department of Epigenetics, Van Andel Research Institute, Grand Rapids, MI, USA

⁴Department of Epigenetics, Max Planck Institute of Immunobiology and Epigenetics, Freiburg, Germany

⁵Institute for Anatomy and Cell Biology, Julius Maximilians University Würzburg, Würzburg, Germany

⁶Institute of Neuroanatomy, University Medical Center Hamburg-Eppendorf, Hamburg, Germany

⁷Department of Ophthalmology, St. Franziskus Hospital, Münster, Germany

Received: 19 September 2024 / Accepted: 11 November 2024

Published online: 14 November 2024

References

1. Yau JWY, Rogers SL, Kawasaki R, Lamoureux EL, Kowalski JW, Bek T, et al. Global prevalence and major risk factors of diabetic retinopathy. *Diabetes Care*. 2012;35:556–64.
2. Saaddine JB. Projection of diabetic retinopathy and other major eye diseases among people with diabetes mellitus: United States, 2005–2050. *Arch Ophthalmol*. 2008;126:1740.
3. Stitt AW, Curtis TM, Chen M, Medina RJ, McKay GJ, Jenkins A, et al. The progress in understanding and treatment of diabetic retinopathy. *Prog Retin Eye Res*. 2016;51:156–86.
4. Agarwal D, Gelman R, Prospero Ponce C, Stevenson W, Christoforidis JB. The vitreomacular interface in diabetic retinopathy. *J Ophthalmol*. 2015;2015:1–10.
5. El Rami H, Barham R, Sun JK, Silva PS. Evidence-based treatment of diabetic retinopathy. *Semin Ophthalmol*. 2017;32:67–74.
6. Wong TY, Haskova Z, Asik K, Bauman CR, Csaky KG, Eter N, et al. Faricimab treat-and-extend for diabetic macular edema. *Ophthalmology*. 2024;131:708–23.
7. Writing Committee for the Diabetic Retinopathy Clinical Research Network, Gross JG, Glassman AR, Jampol LM, Inusah S, Aiello LP, et al. Panretinal photocoagulation vs intravitreal ranibizumab for proliferative diabetic retinopathy: a randomized clinical trial. *JAMA*. 2015;314:2137.
8. Rush RB. One year results of faricimab for aflibercept-resistant diabetic macular edema. *Clin Ophthalmol*. 2023;17:2397–403.
9. Akiba J, Arzabe CW, Trempe CL. Posterior vitreous detachment and neovascularization in diabetic retinopathy. *Ophthalmology*. 1990;97:889–91.
10. Blankenship GW, Machemer R. Long-term diabetic vitrectomy results. Report of 10 year follow-up. *Ophthalmology*. 1985;92:503–6.
11. Boneva SK, Wolf J, Rosmus D-D, Schlecht A, Prinz G, Laich Y, et al. Transcriptional profiling uncovers human hyalocytes as a unique innate immune cell population. *Front Immunol*. 2020;11:567274.
12. Wolf J, Boneva S, Rosmus D-D, Agostini H, Schlunck G, Wieghefer P, et al. Deciphering the molecular signature of human hyalocytes in relation to other innate immune cell populations. *Invest Ophthalmol Vis Sci*. 2022;63:9.
13. Qiao H, Hisatomi T, Sonoda K-H, Kura S, Sassa Y, Kinoshita S, et al. The characterization of hyalocytes: the origin, phenotype, and turnover. *Br J Ophthalmol*. 2005;89:513–7.
14. Boeck M, Thien A, Wolf J, Hagemeyer N, Laich Y, Yusuf D, et al. Temporospatial distribution and transcriptional profile of retinal microglia in the oxygen-induced retinopathy mouse model. *Glia*. 2020;68:1859–73.
15. Wieghefer P, Hagemeyer N, Sankowski R, Schlecht A, Staszewski O, Amann L, et al. Mapping the origin and fate of myeloid cells in distinct compartments of the eye by single-cell profiling. *EMBO J*. 2021;40:e105123.
16. Boneva SK, Wolf J, Hajdú RI, Prinz G, Salié H, Schlecht A, et al. In-depth molecular characterization of neovascular membranes suggests a role for hyalocyte-to-myofibroblast transdifferentiation in proliferative diabetic retinopathy. *Front Immunol*. 2021;12:757607.
17. Jones CH, Gui W, Schumann RG, Boneva SK, Lange CAK, Van Overdam KA, et al. Hyalocytes in proliferative vitreo-retinal diseases. *Expert Rev Ophthalmol*. 2022;17:263–80.
18. Migacz JV, Otero-Marquez O, Zhou R, Rickford K, Murillo B, Zhou DB, et al. Imaging of vitreous cortex hyalocyte dynamics using non-confocal quadrant-detection adaptive optics scanning light ophthalmoscopy in human subjects. *Biomed Opt Express*. 2022;13:1755.
19. Jallili V, Afgan E, Gu Q, Clements D, Blankenberg D, Goecks J, et al. The Galaxy platform for accessible, reproducible and collaborative biomedical analyses: 2020 update. *Nucleic Acids Res*. 2020;48:W395–402.
20. Wolf J, Boneva S, Schlecht A, Lapp T, Auw-Haendrich C, Lagrèze W, et al. The Human Eye Transcriptome Atlas: a searchable comparative transcriptome database for healthy and diseased human eye tissue. *Genomics*. 2022;114:110286.
21. Schnichels S, Paquet-Durand F, Löscher M, Tsai T, Hurst J, Joachim SC, et al. Retina in a dish: cell cultures, retinal explants and animal models for common diseases of the retina. *Prog Retin Eye Res*. 2021;81:100880.
22. Bayik D, Tross D, Haile LA, Verthelyi D, Klinman DM. Regulation of the maturation of human monocytes into immunosuppressive macrophages. *Blood Adv*. 2017;1:2510–9.
23. Zwadlo G, Bröcker EB, von Bassewitz DB, Feige U, Sorg C. A monoclonal antibody to a differentiation antigen present on mature human macrophages and absent from monocytes. *J Immunol*. 1985;134:1487–92.
24. Jousen AM, Poulaki V, Le ML, Koizumi K, Esser C, Janicki H, et al. A central role for inflammation in the pathogenesis of diabetic retinopathy. *FASEB J*. 2004;18:1450–2.
25. Delaby C, Pilard N, Puy H, Canonne-Hergaux F. Sequential regulation of ferroptosis expression after erythrophagocytosis in murine macrophages: early mRNA induction by haem, followed by iron-dependent protein expression. *Biochem J*. 2008;411:123–31.
26. Pfefferlé M, Ingoglia G, Schaer CA, Yalamanoglu A, Buzzi R, Dubach IL, et al. Hemolysis transforms liver macrophages into anti-inflammatory erythrophagocytes. *J Clin Invest*. 2020;130:5576–90.
27. Nairz M, Theurl I, Swirski FK, Weiss G. Pumping iron-how macrophages handle iron at the systemic, microenvironmental, and cellular levels. *Pflugers Arch*. 2017;469:397–418.
28. Bressler SB, Beaulieu WT, Glassman AR, Gross JG, Jampol LM, Melia M, et al. Factors associated with worsening proliferative diabetic retinopathy in eyes

- treated with panretinal photocoagulation or ranibizumab. *Ophthalmology*. 2017;124:431–9.
29. Lange CAK, Stavrakas P, Luhmann UFO, De Silva DJ, Ali RR, Gregor ZJ, et al. Intraocular oxygen distribution in advanced proliferative diabetic retinopathy. *Am J Ophthalmol*. 2011;152:406–e4123.
30. Yao Y, Li R, Du J, Long L, Li X, Luo N. Interleukin-6 and diabetic retinopathy: a systematic review and meta-analysis. *Curr Eye Res*. 2019;44:564–74.
31. Sharma S. Interleukin-6 trans-signaling: a pathway with therapeutic potential for diabetic retinopathy. *Front Physiol*. 2021;12:689429.
32. Agostini H, Abreu F, Bauml CR, Chang DS, G. Csaky K, Demetriades AM, et al. Faricimab for neovascular age-related macular degeneration and diabetic macular edema: From preclinical studies to phase 3 outcomes. *Graefes Arch Clin Exp Ophthalmol*. 2024;online ahead of print.
33. Watanabe D, Suzuma K, Suzuma I, Ohashi H, Ojima T, Kurimoto M, et al. Vitreous levels of angiopoietin 2 and vascular endothelial growth factor in patients with proliferative diabetic retinopathy. *Am J Ophthalmol*. 2005;139:476–81.
34. Loporchio DF, Tam EK, Cho J, Chung J, Jun GR, Xia W, et al. Cytokine levels in human vitreous in proliferative diabetic retinopathy. *Cells*. 2021;10:1069.
35. Wu F, Phone A, Lamy R, Ma D, Laotaweungsawat S, Chen Y, et al. Correlation of aqueous, vitreous, and plasma cytokine levels in patients with proliferative diabetic retinopathy. *Invest Ophthalmol Vis Sci*. 2020;61:26.
36. Wolf J, Rasmussen DK, Sun YJ, Vu JT, Wang E, Espinosa C, et al. Liquid-biopsy proteomics combined with AI identifies cellular drivers of eye aging and disease *in vivo*. *Cell*. 2023;186:4868–e488412.
37. Abd-Elrahman I, Meir K, Kosuge H, Ben-Nun Y, Weiss Sadan T, Rubinstein C, et al. Characterizing cathepsin activity and macrophage subtypes in excised human carotid plaques. *Stroke*. 2016;47:1101–8.
38. Hannaford J, Guo H, Chen X. Involvement of cathepsins B and L in inflammation and cholesterol trafficking protein NPC2 secretion in macrophages. *Obesity*. 2013;21:1586–95.
39. Hausmann M, Obermeier F, Schreiter K, Spottl T, Falk W, Schölmerich J, et al. Cathepsin D is up-regulated in inflammatory bowel disease macrophages. *Clin Exp Immunol*. 2004;136:157–67.
40. Schlecht A, Boneva S, Gruber M, Zhang P, Horres R, Bucher F, et al. Transcriptomic characterization of human choroidal neovascular membranes identifies calprotectin as a novel biomarker for patients with age-related macular degeneration. *Am J Pathol*. 2020;190:1632–42.
41. Wang S, Song R, Wang Z, Jing Z, Wang S, Ma J. S100A8/A9 in inflammation. *Front Immunol*. 2018;9:1298.
42. Cesaro A, Anceriz N, Plante A, Pagé N, Tardif MR, Tessier PA. An inflammation loop orchestrated by S100A9 and calprotectin is critical for development of arthritis. Bobé P. Editor *PLoS ONE*. 2012;7:e45478.
43. Fan Y, Zhang J, Cai L, Wang S, Liu C, Zhang Y, et al. The effect of anti-inflammatory properties of ferritin light chain on lipopolysaccharide-induced inflammatory response in murine macrophages. *Biochim Biophys Acta*. 2014;1843:2775–83.
44. Ciudin A, Hernández C, Simó R. Iron overload in diabetic retinopathy: a cause or a consequence of impaired mechanisms? *Exp Diabetes Res*. 2010;2010:714108.
45. Boneva SK, Wolf J, Wieghofer P, Sebag J, Lange CA. Hyalocyte functions and immunology. *Expert Rev Ophthalmol*. 2022;17:249–62.
46. Hamburg A. Some investigations on the cells of the vitreous body. *Ophthalmologica*. 1959;138:81–107.
47. Knutson M, Wessling-Resnick M. Iron metabolism in the reticuloendothelial system. *Crit Rev Biochem Mol Biol*. 2003;38:61–88.
48. Oldenborg P-A, Zheleznyak A, Fang Y-F, Lagenaur CF, Gresham HD, Lindberg FP. Role of CD47 as a marker of self on red blood cells. *Science*. 2000;288:2051–4.
49. Kelley SM, Ravichandran KS. Putting the brakes on phagocytosis: don't-eat-me signaling in physiology and disease. *EMBO Rep*. 2021;22:e52564.
50. Schulz A, Wahl S, Rickmann A, Ludwig J, Stanzel BV, Von Briesen H, et al. Age-related loss of human vitreal viscoelasticity. *Trans Vis Sci Tech*. 2019;8:56.

Publisher's note

Springer Nature remains neutral with regard to jurisdictional claims in published maps and institutional affiliations.